



Entomoneis grisslehamnensis, a New Diatom (Bacillariophyceae) from the Baltic Coast of Sweden with taxonomic and ecological notes on *Entomoneis paludosa* (W. Smith) Reimer

Adil Y. Al-Handal, Maja Mucko, Petra Peharec Štefanić & Angela Wulff

To cite this article: Adil Y. Al-Handal, Maja Mucko, Petra Peharec Štefanić & Angela Wulff (2023): *Entomoneis grisslehamnensis*, a New Diatom (Bacillariophyceae) from the Baltic Coast of Sweden with taxonomic and ecological notes on *Entomoneis paludosa* (W. Smith) Reimer, Diatom Research, DOI: [10.1080/0269249X.2023.2215110](https://doi.org/10.1080/0269249X.2023.2215110)

To link to this article: <https://doi.org/10.1080/0269249X.2023.2215110>



© 2023 The Author(s). Published by Informa UK Limited, trading as Taylor & Francis Group.



[View supplementary material](#)



Published online: 04 Jul 2023.



[Submit your article to this journal](#)



[View related articles](#)



[View Crossmark data](#)

Entomoneis grisslehamnensis, a New Diatom (Bacillariophyceae) from the Baltic Coast of Sweden with taxonomic and ecological notes on *Entomoneis paludosa* (W. Smith) Reimer

ADIL Y. AL-HANDAL ^{1*}, MAJA MUCKO ², PETRA PEHAREC ŠTEFANIĆ ² & ANGELA WULFF ¹

¹Department of Biological and Environmental Sciences, University of Gothenburg, Gothenburg, Sweden

²Department of Biology, Faculty of Science, University of Zagreb, Zagreb, Croatia

The diatom genus *Entomoneis* includes species with panduriform frustules characterized by a bilobate, elevated keel, sigmoid raphe canal and numerous open, porous girdle bands. During a phytoplankton survey along the Baltic coast of Sweden, we observed numerous *Entomoneis* cells, some belonging to the well-known *Entomoneis paludosa*, while others remained unknown. Morphological and ultrastructural studies of the unknown species were performed with light microscopy (LM), scanning (SEM) and transmission (TEM) electron microscopy, and revealed a unique set of morphological characters. Live cells of *Entomoneis grisslehamnensis* sp. nov. contain one plate-like plastid and show various degrees of torsion about the apical axis. Microscopic features of cleaned frustules are discussed in comparison with similar species. Most importantly, every 2nd to 5th virga is strongly elevated, uniseriate striae are composed of quadrangular areolae with finely perforated hymenes; the winged keel with a discernible raphe canal is structurally strengthened by raphe fibulae with a flattened wing area, and the main part of the valve bulges towards the margins; striation is decussate on the wings and there is one row of raphe canal areolae at the central area. In addition to describing this new species of an underappreciated, yet cosmopolitan diatom genus, we contribute to the taxonomy of *E. paludosa* with LM, SEM and TEM details, some of which were not sufficiently noted in original descriptions or re-examination of type material and other specimens made by Dalu et al. [2015. A re-examination of the type material of *Entomoneis paludosa* (W. Smith) Reimer and its morphology and distribution in African waters. *Fottea* 15: 11–25] and Long et al. [2022. Ultrastructure of three species of *Entomoneis* (Bacillariophyta) from Lake Qinghai of China, with reference to the external areola occlusions. *PhytoKeys* 189: 29–50. doi:10.3897/phytokeys.189.78149].

Keywords: *Entomoneis*, morphology, new species, panduriform, *E. paludosa*

Introduction

The genus *Entomoneis* Ehrenberg belongs to a group of diatoms characterized by a discernibly panduriform (constricted in the middle) frustule with a sigmoid raphe canal enclosed in the elevated bilobate (winged) keel, numerous open, porous girdle bands, often showing frustule torsion around the apical and/or transapical axis (Patrick & Reimer 1975, Round et al. 1990, Mejdandžić et al. 2017, Mejdandžić et al. 2018). These shared morphological features can be well observed in LM, however, electron microscopy (both SEM and TEM for very fine details) reveals a range of genus- and/or species-specific features. The most important are: (i) the shape or line of transition between the valve body and winged keel (previously called ‘junction line’); (ii) presence and organization of various kinds of fibulae (basal, keel [frequently termed intermedial] and raphe) with frequent fusion (H, W or Y shapes); (iii) variety of areola shapes (round, elliptical, elongated,

teardrop, quadrangular; occluded or not by finely perforated hymenes or by more strongly silicified vela); (iv) presence of hymenate strip-like striae with fine round or linear perforations in lightly silicified species (mostly planktonic marine species). Some features are restricted to one or a few species, such as (i) an obliquely transapical fascia (e.g., *E. annagodheae* Al-Handal & Mucko); (ii) silica thickenings between girdle band areolae (e.g., *E. pusilla* Bosak & Mejdandžić); (iii) bulged cell compartments (e.g., *E. triundulata* Bing Liu & Williams); (iv) silica spines beside the central nodule (e.g., *E. centrospinosa* Osada & Kobayasi) (Patrick & Reimer 1975, Osada & Kobayasi 1991, Liu et al. 2018, Mejdandžić et al. 2018, Al-Handal et al. 2020). Altogether, these features increase the morphological complexity of the valve and make this small genus challenging to investigate (Osada & Kobayasi 1990b, Clavero et al. 1999, Liu et al. 2018, Mejdandžić et al. 2018, Al-Handal et al. 2020, Long et al. 2022).

*Corresponding author. E-mail: adil.yousif@bioenv.gu.se

Associate Editor: Aleksandra Zgrundo

(Received 24 August 2022; accepted 15 March 2023)

© 2023 The Author(s). Published by Informa UK Limited, trading as Taylor & Francis Group.

This is an Open Access article distributed under the terms of the Creative Commons Attribution License (<http://creativecommons.org/licenses/by/4.0/>), which permits unrestricted use, distribution, and reproduction in any medium, provided the original work is properly cited. The terms on which this article has been published allow the posting of the Accepted Manuscript in a repository by the author(s) or with their consent.

In his publication on taxonomically accepted species and nomenclatural names in databases (AlgaeBase and DiatomBase), Williams (2021) questioned the number of taxonomically accepted species belonging to *Entomoneis* and *Amphiprora*. Using Williams' criteria, there are currently 32 taxonomically accepted *Entomoneis* species, seven accepted varieties and one forma in AlgaeBase.

On the other hand, a quick search through DiatomBase reveals smaller number of accepted species (19; with two varieties), and closer examination indicates that DiatomBase does not include the latest research (i.e., species described in 2017: *E. tenera* Mejdandžić & Bosak 2018; *E. pusilla*; 2022: *E. sinensis* Bing Liu & Williams and *E. qinghainensis* Bing Liu & Williams). However, using 'extant' search in DiatomBase, more records appear (total of 52), including previously mentioned taxonomically accepted species described in the last five years, although they are not denoted as 'accepted'. Nevertheless, for purposes of this study, as with previous ones published by Al-Handal *et al.* (2020) and Mejdandžić *et al.* (2017, 2018), we follow AlgaeBase's number of 32 taxonomically accepted species in *Entomoneis* (Guiry & Guiry 2023). Of course, the taxonomic status of every species can be questioned, while some of the names are nomenclatural transfers from *Amphiprora* Ehrenberg, so statements of the exact number of different and accepted species in *Entomoneis* must be taken with caution.

Based on previously published descriptions of *Entomoneis* taxa, and re-examination of type material, *Entomoneis* is found in freshwater, brackish and marine environments, inhabiting both the plankton and benthos (epiphyton, epipelon and epilithon). The assumption that the keeled raphe canal present in the Bacillariales Hendey, Rhopalodiales D.G.Mann and Surirellales D.G.Mann (Round *et al.* 1990, Ruck & Theriot 2011) is an evolutionary adaptation to enhance motility efficiency (Round 1981, Lowe 2003) is controversial. There are several keel-bearing species that either float in the pelagic or survive epiphytically, where motility does not seem advantageous, and furthermore, not all keeled raphe-bearing diatoms are epipellic, where active movement is beneficial (John 1983, Osada & Kobayasi 1985, 1990a, 1990b, 1990c, 1991, Clavero *et al.* 1999, Reinke & Wujek, 2013, Paillès *et al.* 2014, Mejdandžić *et al.* 2017, Liu *et al.* 2018, Mejdandžić *et al.* 2018). We know from previous research that the percentage of taxonomically accepted *Entomoneis* species found primarily in the plankton is constantly increasing (about 25%): *E. tenera*, *E. pusilla*, *E. gracilis* Mejdandžić & Bosak, *E. vilicicii* Bosak & Mejdandžić, *E. infula* Mejdandžić & Bosak, *E. adriatica* Mejdandžić & Bosak, *E. umbratica* Mejdandžić & Bosak and *Entomoneis aneghodeae* (Mejdandžić *et al.* 2017, Mejdandžić *et al.* 2018, Al-Handal *et al.* 2020). Overall, these most recent findings of planktonic *Entomoneis* species corroborate their underappreciation and neglect in general plankton studies. *Entomoneis paludosa* (W. Smith)

Reimer, originally described as a benthic, fresh to slightly brackish water species, is also commonly found in the plankton, and in marine environments (Hällfors, 2004, Mucko, M. unpublished data). Knowledge on the distribution and abundance of *Entomoneis* species is still scarce however, although taxonomical studies documenting *Entomoneis* taxa in planktonic and benthic samples around the world are becoming more precise and easier.

Distribution and abundance data of *Entomoneis* in Swedish coastal regions are limited. In his study on samples collected over a nine-year period (1974–1983), Kuylenstierna (1990) reported seven species of *Entomoneis* (as *Amphiprora*) from the west coast of Sweden. Similar numbers were also recorded from the Baltic Sea (Hällfors 2004). Subsequently, a new planktonic *Entomoneis*, *E. annagodheae* (Al-Handal *et al.* 2020) was described from the Swedish west coast. However, in the most recent phytoplankton surveys along the Baltic coast of Sweden, numerous *Entomoneis* cells were observed, of which those with pronounced virgae and silica thickenings around the areolae were observed in two locations, Grisslehamn and Juniskär. SEM examination of these cells revealed some unique ultrastructural features, allowing us to describe it as *Entomoneis grisslehamnensis* sp. nov. A comparison based on LM, SEM and TEM observations between *E. grisslehamnensis* and other known *Entomoneis* taxa is provided.

The phytoplankton samples also contained a considerable number of *E. paludosa* cells, which allowed us to contribute new images and measurements, increasing the ultrastructural knowledge of this species. This paper represents the third study of newly recorded *E. paludosa* specimens in the last decade, adding to information from Dalu *et al.* (2015) and Long *et al.* (2022). An older but no less important contribution was made by Osada & Kobayasi (1990c) alongside an ultrastructural examination of *E. punctulata* (Grunow) Osada & Kobayasi and *E. pseudoduplex* Osada & Kobayasi (Osada & Kobayasi 1990c). Osada & Kobayasi (1990c) studied specimens collected in a river, an estuary and a pond (Mookoppe-gawa River; Ara-kawa estuary and Hinuma Pond, Japan), Dalu *et al.* (2015) re-examined W. Smith's type material and newly collected material from the Kowie River, South Africa, while Long *et al.* (2022) studied material from the slightly brackish Lake Qinghai, China. To our knowledge, we present the first detailed examination of *E. paludosa* material from the Baltic Sea, from brackish to marine conditions, the highest salinity compared to other published studies.

Material and methods

Sample collection

During a diatom survey along the Swedish coast of the Baltic, cells of *E. grisslehamnensis* were found in two

locations: Grisslehamn (60° 4,63275' N, 18° 49,51328' E), and Juniskär (62° 17,67714' N, 17° 26,93924'E). These sites are located 114 and 367 km north of Stockholm, respectively. The coast is characterized by an archipelago of very small, scattered islets, hundreds of metres from land. Salinity in these regions is lowered by freshwater discharge from small streams from the adjacent forests. Sampling was carried out on 21st May 2019 from Juniskär and on 22nd May from Grisslehamn. Benthic samples (also containing *E. paludosa*) were obtained by scraping the littoral sediment surface covered by a thin layer of water into 50 ml plastic tubes. For the study of epiphytic diatoms several macrophytes were also collected from various parts of the study area and kept in plastic bags. To allow examination of living cells, no fixatives were added in the field. All collected samples were stored in a car-battery operated refrigerator box.

Treatment of samples

Sediment samples were rinsed with deionized water before boiling in 35% hydrogen peroxide to digest all organic material. While still hot, a few drops of 50% hydrochloric acid were added to the samples to remove any remaining carbonates. After several rinses with deionized water, 0.2 ml of the cleaned diatom material was placed on a cover slip and left to dry at room temperature. Permanent slides were made by mounting in Naphrax. For epiphytic material, parts of the macrophytes were placed in 50 ml glass beakers containing distilled water and shaken to free all loosely attached cells. The aliquot containing diatoms was then treated as above.

For LM, several slides were prepared from each sample to study the frequency of species occurrences, variation in morphometric measurements and imaging using a Zeiss Axioimager 2 LM with differential interference contrast objectives (DIC) and a Canon Powershot 14 camera (Department of Biological and Environmental Sciences, University of Gothenburg, Sweden). For SEM, the cleaned diatoms were filtered on 1 µm Nucleopore Whatman filters and left to dry on an aluminium stub covered with conductive black carbon disks before coating with gold palladium. A Zeiss Ultra 55 FEG SEM (Chalmers University, Sweden) was used for valve ultrastructural examination and imaging.

The relative abundance of *E. grisslehamnensis* in plankton samples was estimated following Utermöhl sedimentation and counting (Utermöhl 1931, 1958). For TEM examination, cleaned material was directly deposited onto Formvar-carbon coated copper grids, air dried and examined with a FEI Morgagni 268D microscope (Eindhoven, The Netherlands) operated at 70 kV. Images were taken with an incorporated side-mounted CCD Camera (Mega View III from Soft Imaging System Co.), and subsequent image analysis used CorelDRAW Graphics Suite (v. X8,

Corel Corporation, Ottawa, Ontario). The terminology followed Ross et al. (1979), Paddock & Sims (1981), Round et al. (1990) and Osada & Kobayasi (1985).

Results

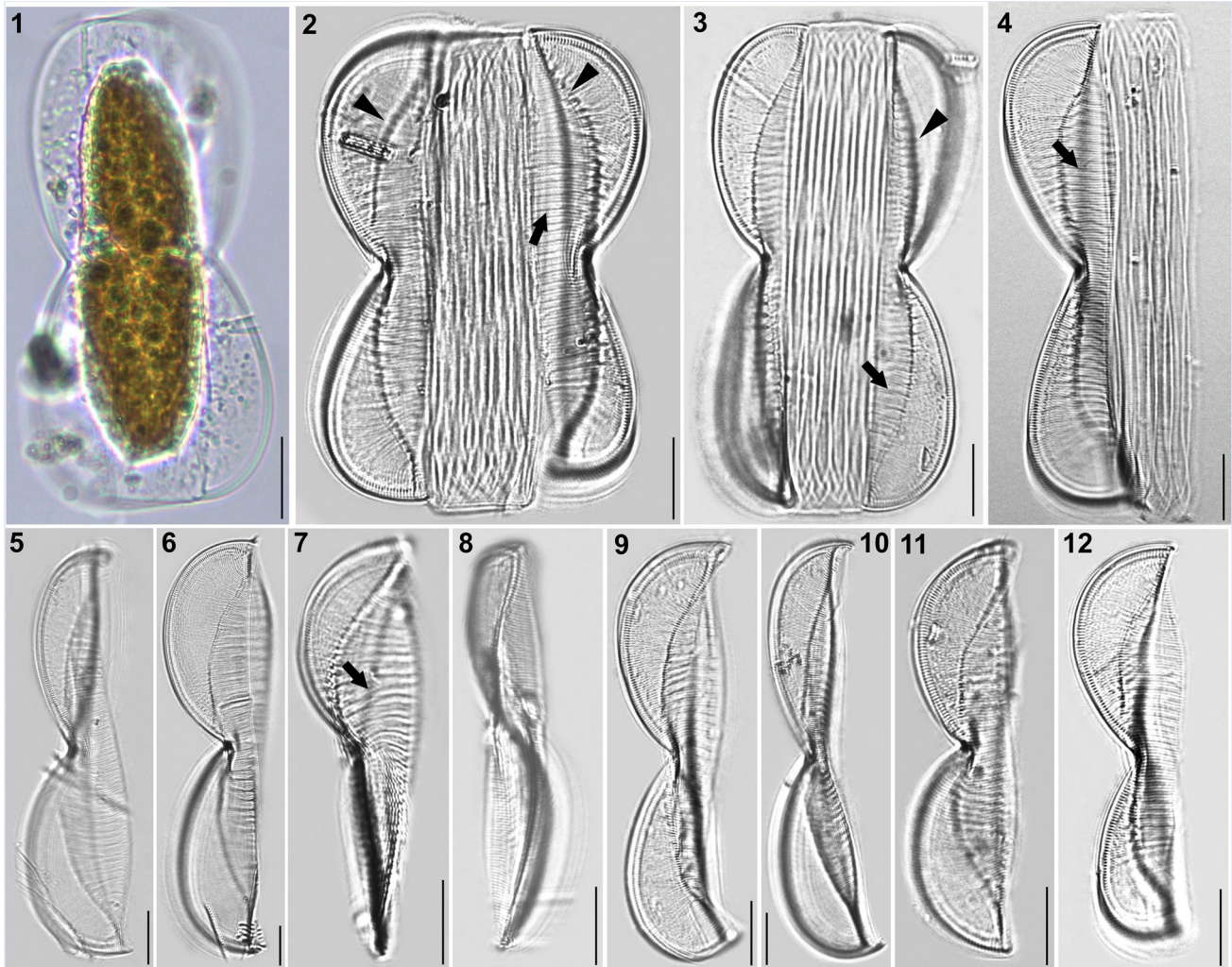
Entomoneis grisslehamnensis Al-Handal, Mucko & Wulff sp. nov. (LM Figs 1–12, SEM Figs 13–27)

Description

Light microscopy (LM): Cells solitary and well silicified. One plate-like plastid per cell (Fig. 1). Frustules panduriform in girdle view, deeply constricted in the middle with numerous crossed, open girdle bands (Figs 2–4). Frustules often twisted about apical axis, with various degrees of torsion (Figs 3, 7, 8). Valves linear to linear-lanceolate, 43–124 µm long, 6–11 µm wide at their constriction, 12–22 µm at widest area, including wings ($n = 47$). Valve apices scalpelliform in girdle view (Figs 5–12), acutely rounded in valve view (Fig. 7). Raphe-bearing keel sigmoid in valve view, very well pronounced, with raphe fibulae (Figs 6, 11, 12, 24–27 fibulae in 10 µm). Transition between valve body and elevated winged keel is arcuate in girdle view, with a row of basal fibulae from the apex to the constricted centre (Figs 2, 3, arrowheads). Transapical striae appear decussate at winged keel (because of radial orientation; Figs 2, 4, 9, 10, 11) parallel on valve body (Figs 2–7). Striae very dense, not discernible in LM, with pronounced thickened elevated virgae every 2–5 striae (Figs 2–4, 7, arrows; 10–14 elevated virgae in 10 µm).

Electron microscopy (EM): Frustules panduriform in girdle view, with strong middle constriction (Fig. 13, larger specimen; Figs 14, 15, smaller specimen). Winged keel with discernible raphe canal structurally reinforced with raphe fibulae (Figs 15–17); with laterally flattened wing area and wider valve body (Figs 14, 15). Frustule surface smooth, with the exception of randomly spaced, elevated, more silicified virgae on valve body (every 2–5 striae; Figs 17–19). Elevated virgae more silicified towards valve margins (Figs 19, 22). Transapical striae are fine and dense, uniseriate, 38–42 in 10 µm (Figs 13–20). Striae are parallel on valve body and radial on winged keel, appearing decussate when two apical sides are flattened in keel area (Figs 14, 16, 20, 23, 26). Areolae dense, quadrangular, evenly distributed in transapical lines and occluded by finely perforated hymenes, 70–74 in 10 µm (Figs 24–26). Elevated, more silicified margins of quadrangular areolae (i.e., silicified rim) scattered on wings (Figs 24–27).

Raphe-bearing keel is narrow and elevated, sigmoid with different degrees of torsion (Figs 17, 18). Striae extend to the raphe canal, usually with 3–4 areolae per long striae (Figs 20, 23, 25), with the addition of one row of smaller round areolae in the central area (Figs 19, 24, arrows). Raphe canal narrow and elevated, central node with simple proximal raphe endings (Figs 18, 19), Terminal raphe



Figs 1–12. LM micrographs of *Entomoneis grisslehamnensis* sp. nov. at different focal planes. Fig. 1. Live cell in girdle view showing panduriform frustule and plate-like plastid. Figs 2–4. Panduriform frustule with elevated virgae on valve body (arrows), basal fibulae forming arcuate transition between bulged valve body and flattened wing (arrowheads) and numerous crossed girdle bands. Figs 5–6. Valves in girdle view showing scalpelliform apices. Figs 7–8. Apically torsioned valves. Figs 9–12. Valves in girdle view with pronounced raphe fibulae and elevated virgae on valve body. Scale bar = 10 µm.

endings are deflected towards the ventral side and terminate in helictoglossae (Figs 18, 21, inner arrow). Cingulum is composed of 7–8 crossed, narrow and open bands, each band perforated by transversally elongated areolae with finely perforated hymenes (Figs 13–15).

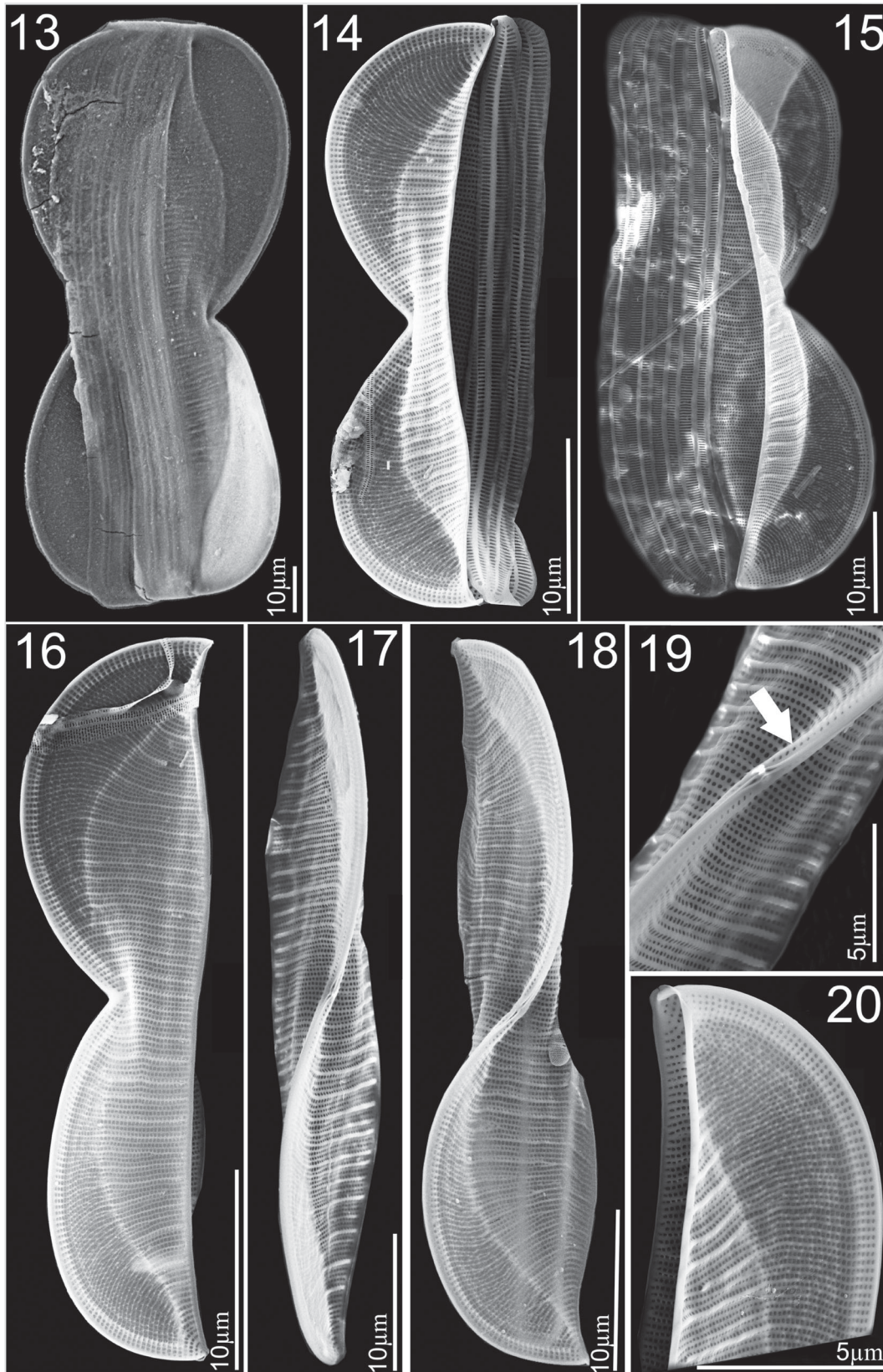
Holotype: Permanent slide and preserved material containing *E. grisslehamnensis* sp. nov. are deposited in the Botanischer Garten und Botanischer Museum (BGBM), Berlin, Germany under accession B 40 0045157. Phycobank registration number: <http://phycobank.org/102935>. Holotype illustrated in Figs 6–8.

Isotype: Permanent slide and cleaned material containing frustules of *E. grisslehamnensis* sp. nov., deposited in the Croatian National Diatom Collection, University of Zagreb, Croatia under accession number HRNDC001665.

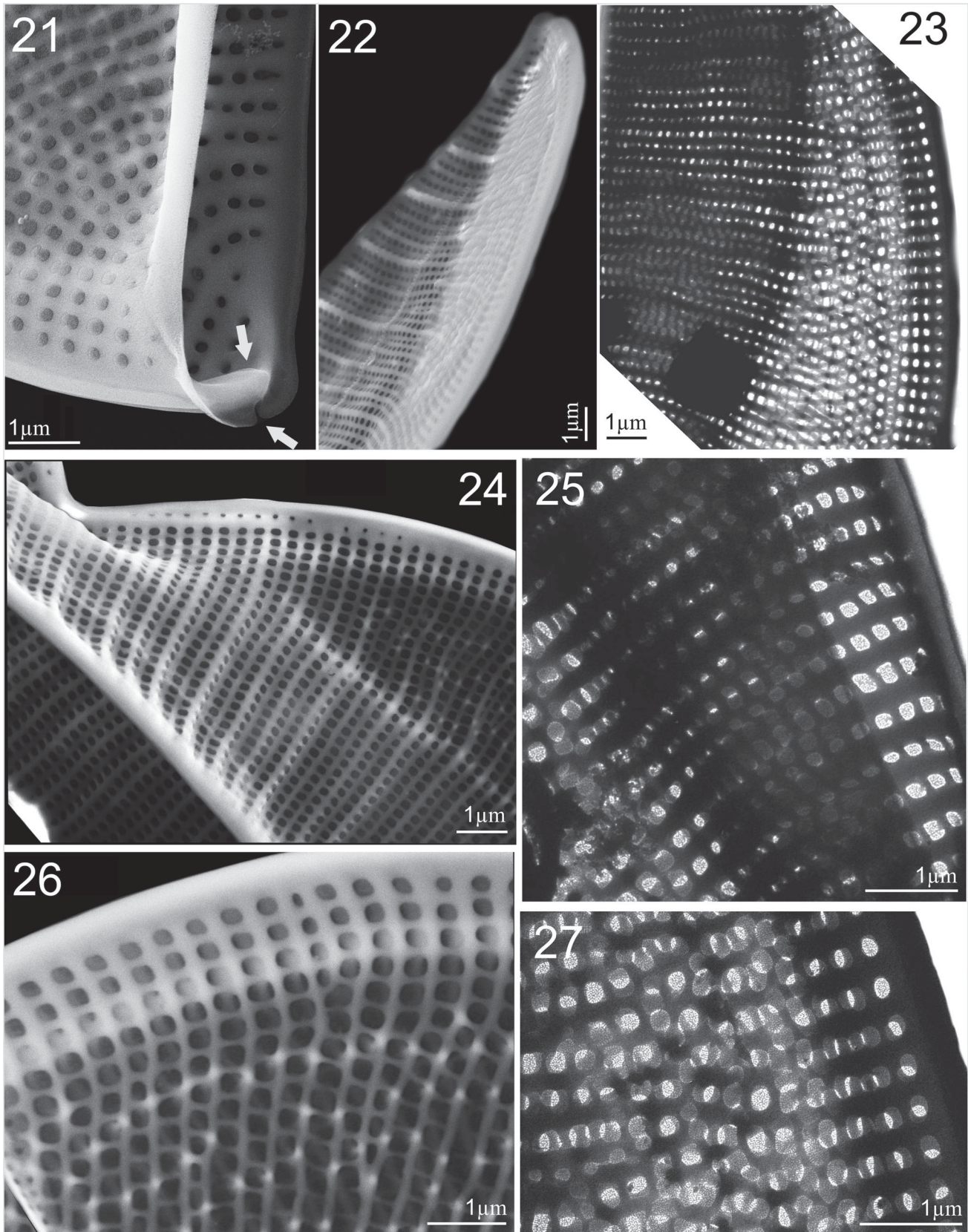
Type locality: Grisslehamn, Baltic coast of Sweden (60° 46' 32" N, 18° 49' 51" E).

Etymology: The epithet refers to the location where the species was found, Grisslehamn.

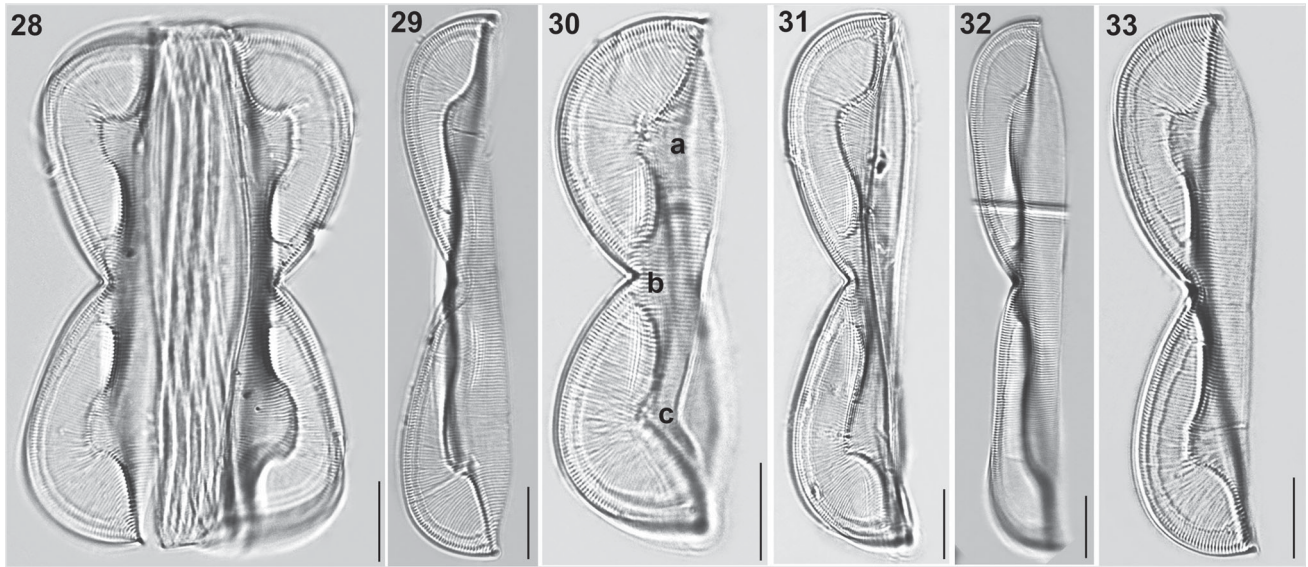
Ecology: *Entomoneis grisslehamnensis* was rarely found on muddy to silty sediment and epiphytic on the brown macrophyte *Mesogloia* sp. (1.2% frequent as benthic and 0.6% as epiphyte). Salinity at time of material collection was 4.9 and water temperature 12.3°C. Associated taxa, which appeared in moderate to high cell frequencies in the samples, were *E. paludosa* (W. Smith) Reimer (2.3%), *Licmophora ehrenbergii* (Kützinger) Grunow (15.6%), *Diatoma elongata* (Lyngbye) C. Agardh (20.1%), *Diatoma tenuis* C. Agardh (6.4%) and *Diatoma vulgare* Bory (5.8%). Another population with smaller individuals of *E. grisslehamnensis* was encountered further north in Juniskär (62°



Figs 13–20. SEM micrographs of *Entomoneis grisslehamnensis* sp. nov. Fig. 13. Frustule in girdle view. Figs 14–15. Valves in girdle view with girdle band details showing bulged valve body and flattened wings with pronounced elevated virgae and silicified rims on wings. Fig. 16. Valve in girdle view with arcuate transition between bulged valve body and flattened wing. Figs 17–18. Valves in valve view with sigmoid raphe canal on elevated keel. Fig. 19. Details of proximal raphe endings in central node. Fig. 20. Scalpelliform valve apex.



Figs 21–27. SEM and TEM micrographs of *Entomoneis grisslehamnensis* sp. nov. Figs 21, 22, 24 and 26. SEM; Figs 23, 25, 27. TEM. Fig. 21. Distal raphe ending (arrow) viewed from inner valve. Fig. 22. Tilted valve apex showing elevated virgae, thicker at the valve margin. Fig. 23. Elevated wing with radial striae appearing decussate. Fig. 24. Bulged valve body and flattened wing with silicified rims around areolae; specific row of areolae on raphe-canal. Figs 25–27. Details of quadrangular areolae perforated with finely perforated hymen.



Figs 28–33. LM micrographs of *Entomoneis paludosa* at different focal planes. Fig. 28. Panduriform frustule in girdle view with sinusoid transition between valve body and keel, pronounced raphe canal and fibulae and numerous crossed girdle bands. Figs 29–33. Different valve sizes viewed in girdle view showing differences in sinusoid curvature of transition between valve body and keel. Scale bar = 10 μ m.

17,67714' N, 17° 26,93924' E). At this location, cells of *E. grisslehamnensis* were only found on the sediment where salinity was lower (1.3) due to mixing with freshwater discharge from streams.

Comparison with similar species: Although *E. grisslehamnensis* possesses some unique morphological characters for *Entomoneis* (i.e., elevated virgae, quadrangular areolae with silicified rim, pronounced narrow raphe-canal with 3–4 areola per long striae), a comparison of morphometric features with similar species is given in Table 1.

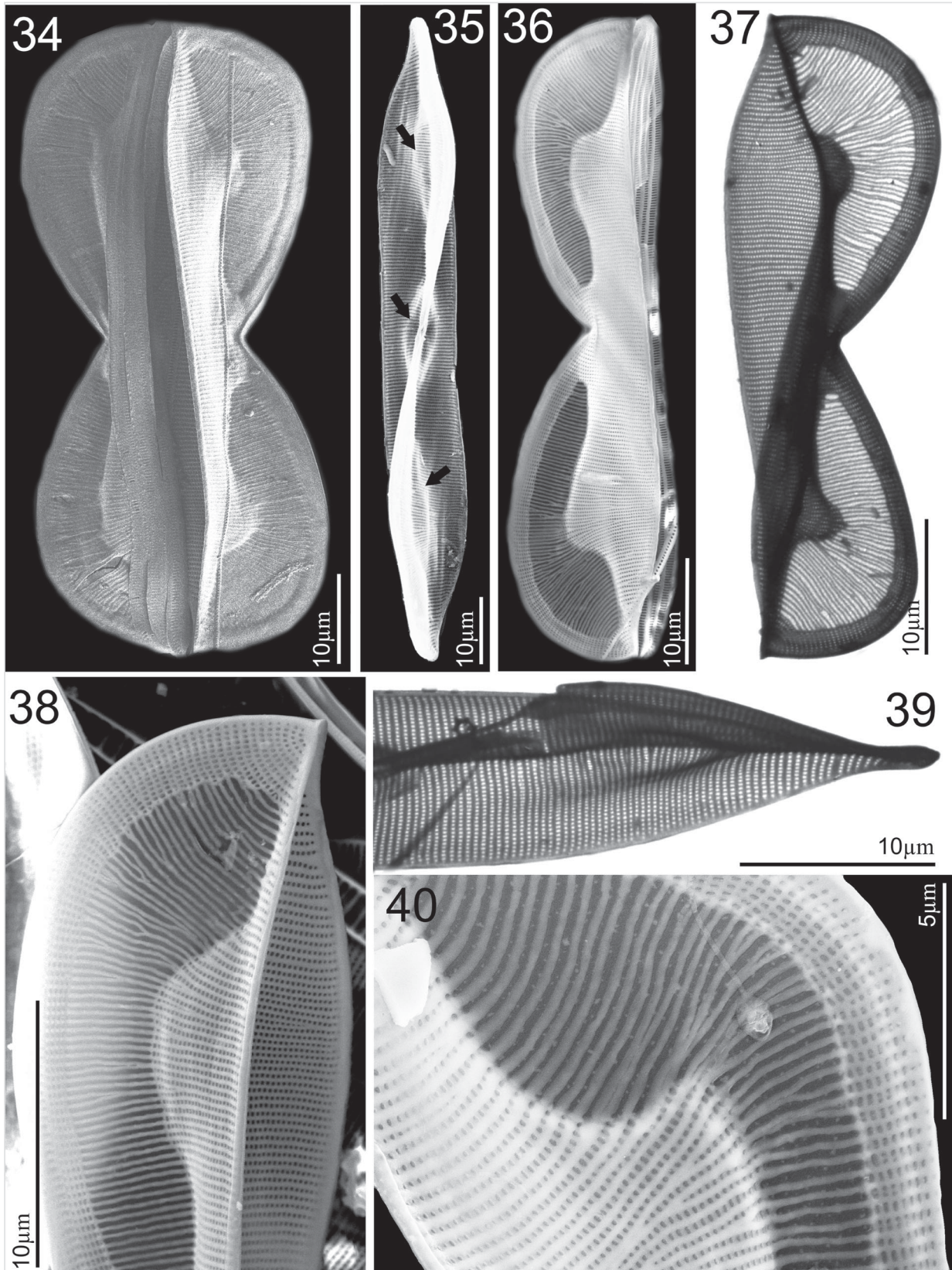
Examination of *Entomoneis paludosa* cells (LM Figs 28–33, SEM Figs 34–50)

Description

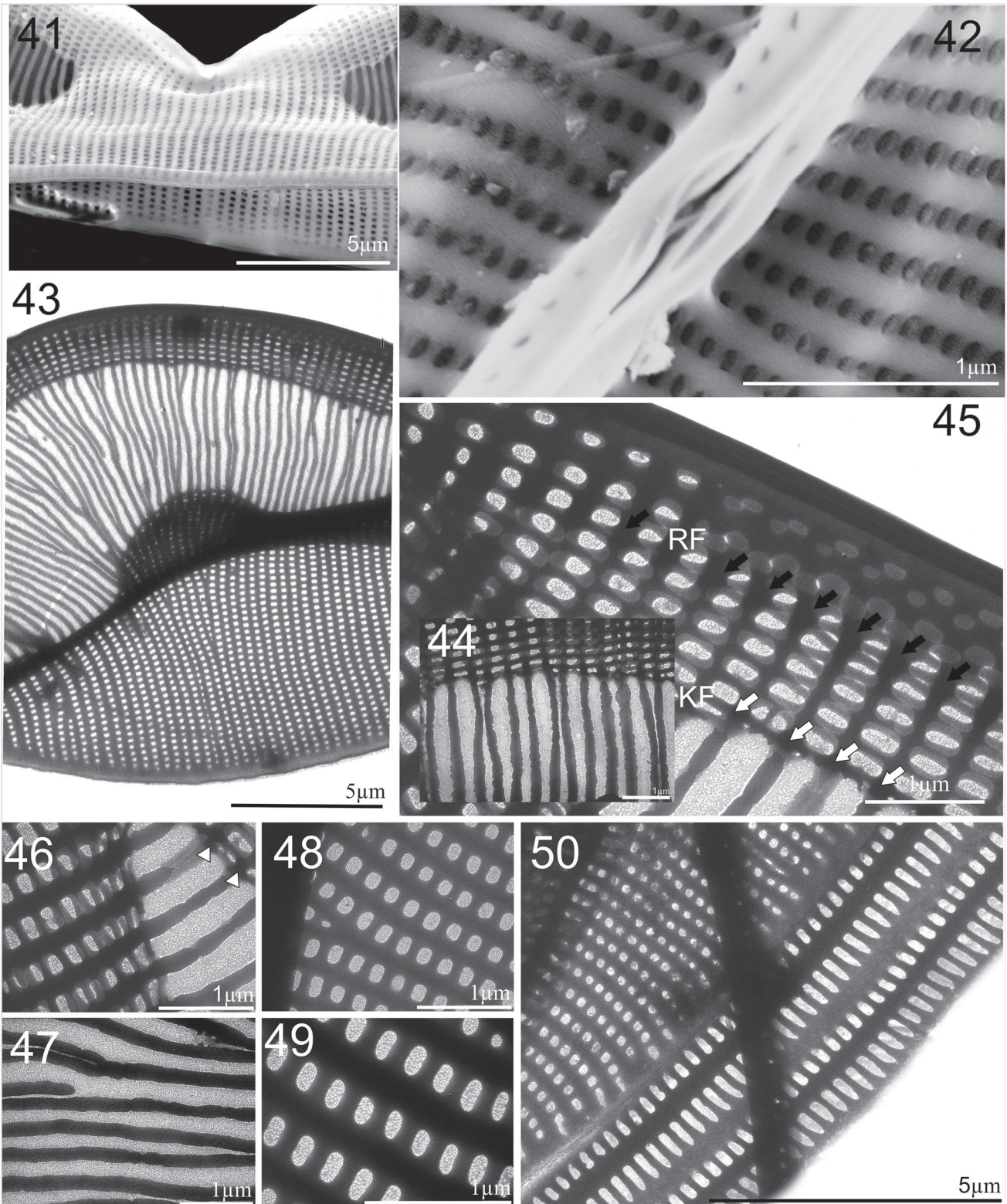
Light microscopy (LM): Cells solitary and well silicified. Frustules panduriform in girdle view and deeply constricted in the middle with numerous crossed girdle bands (Fig. 28). Cells in girdle view with two lunate lobes and broad-scalpelliform apices, 85–120 μ m long ($n = 56$), 10–12 μ m wide in constricted area and 12–16.5 μ m in widest part including wings. Transition between valve body and elevated winged keel distinctly lobed (sinusoid), with various degrees of curvature, depending mostly on cell size (Figs 28–33). Valve body has distinct bulges forming in each wing, as a result of the flattening of the frustule in winged area (Figs 28–33). Depending on the focal plane, a third bulge can appear at the valve centre of smaller specimens (Fig. 30a, b, c bulges). Transapical striae very dense, parallel on valve body, radial on wing (Figs 30,

33; 23–25 striae in 10 μ m). Raphe canal with pronounced raphe fibulae, 24–27 in 10 μ m (Figs 29, 30, 32).

Electron microscopy (EM): Valves linear to linear-lanceolate (Fig. 35) with broad-scalpelliform apices in girdle view (Fig. 38), protracted in valve view (Figs 35, 39). Raphe-bearing keel narrow and sigmoid (Fig. 35). Winged keel is externally perforated, with 7–8 elliptical areolae in central part, and up to 15 elliptical areolae at the cell apices, forming regular transapical striae (Figs 34, 36, 37, 38, 40). These striae continue towards to comb-like hymenate striae (i.e., ricas in Osada & Kobayasi, 1990c; Figs 36, 37, 38, 40). Winged keel body flattened in the area extending from raphe-canal to end of the comb-like ricas (Figs 36, 38, 40). Three bulges in the valve body can be seen in valve view: one surrounding the central nodule and two corresponding to the valve body along the transition to the flattened wing (Fig. 35, arrows). Central area bulge and slight depression around the central nodule and mostly constricted part of panduriform frustule are best observed when the cell is tilted (Fig. 41). These valve bulges differ in size and shape depending on the transition outline (Figs 34, 36–38). Proximal raphe endings deflected to opposite sides, ending simple in elongated slit (Fig. 42). Transition between valve body and winged keel is sinusoid, but bent to various degrees (Figs 34, 36–38, 40). Area of the wing between the transition from valve body to keel and raphe canal is ornamented with a comb-like structure, continuous radial transapical striae with finely perforated hymenes (ricas) and virgae which are often bifurcated (Figs 38, 40, 43, 44, 47). This comb-like structure with hymenate striae ends on the wing at the keel fibulae. Transapical striae on the keel



Figs 34–40. SEM and TEM micrographs of *Entomoneis paludosa*. Figs 34, 35, 36, 38 and 40. SEM; Figs 37 and 39. TEM. Fig. 34. Frustule in girdle view showing sinusoid transition between valve body and keel, pronounced raphe canal and numerous intercalary bands. Fig. 35. Linear to lanceolate valve with three distinctive bulges (arrows). Figs 36 and 37. Valves in girdle view with distinctive sinusoid transition from valve body to keel viewed in SEM (Fig. 36) and TEM (Fig. 37). Figs 38 and 40. Close-up of wing showing regular areolar striae and comb-like structure made from hymenated striae. Fig. 39. Protracted valve apex with areolae details.



Figs 41–50. SEM and TEM micrographs of *Entomoneis paludosa*. Figs 41 and 42. SEM; Figs 43–50. TEM. Fig. 41. Tilted central valve showing flattened wing at the central node and bulged valve body. Fig. 42. Proximal raphe endings and raphe canal areolae. Fig. 43. Details of striation in the wing and valve body. Figs 44 and 45. Close-up of raphe canal striae, raphe fibulae (RF) and keel fibulae (KF) with comb-like striae continuing towards transition between keel and valve body (Fig. 44.). Figs 46–49. Details of perforations in elliptical areolae and comb-like hymenated striae. Fig. 50. Valve margin with valvocopulae ultrastructure showing smaller advalvar and larger abvalvar elongated areolae.

Table 1. Morphological features of *Entomoneis grisslehamnensis* sp. nov. compared to similar species: *E. decussata*, *E. aequabilis*, *E. paludosa*, *E. tenera* and *E. punctulata*.

Feature	Similar species					New species	
	<i>E. decussata</i> (Grunow) Osada & Kobayasi	<i>E. aequabilis</i> (Grunow) Osada & Kobayasi	<i>E. paludosa</i> Osada & Kobayasi	<i>E. tenera</i> Mejdandžić & Bosak	<i>E. punctulata</i> Osada & Kobayasi	<i>E. grissleham-</i> <i>nensis</i> sp. nov.	
Frustule (LM)	deeply constricted, valves narrow, striae visible, strongly decussate on wings	deeply constricted, longitudinally twisted, striae visible, decussate on wings	deeply constricted, keels torsioned, highly arched, striae visible	deeply constricted, often twisted, valves broad, striae invisible	deeply constricted, striae invisible, valve wings broad	deeply constricted, valves broad, striae visible, weakly decussate on wings	
Valve	length (μm)	40–66	47–57	40–130	11–22	18–53	43–124
	width (μm)	7–12	7–9	20–50	3–7	10–19	6–22
	outline	linear to lanceolate	linear, weakly sigmoid	broadly linear	broadly lanceolate	broadly linear	linear to linear lanceolate
Striae	Apex (valve view)	acute, slightly bent to opposite sides	broad scalpelliform	acute, straight	scalpelliform	acute	scalpelliform
	density in 10 μm structure	22–26	32–37	21–26	30–50	34–36	28–42
Areolae		biseriate, decussate on wings in girdle view	biseriate, decussate on wings in girdle view	uniseriate, parallel, separated by raised virgae externally	biseriate, parallel, virgae simple, some bifurcated at valve margin	biseriate, parallel	uniseriate, parallel, virgae often bifurcate, appear decussate on the wing in EM
		slit-like	irregular slit-like, distant	elliptical, poroid	hymenated striae with narrow, elongated perforations in two rows	slit-like	quadrangular, evenly distributed
Transition between valve body and keel		arcuate	np	sinusoid	straight to slightly arcuate	arcuate, restricted to the apical corner	arcuate
Fibulae	basal	close to each other	np	np	born on each wing virgae, sometimes interconnected in shape of H or W	restricted to apical corner	from valve apex to frustule constricted centre
	keel raphe	on keel costae nd	np on keel margin	np nd	np 29–40/10 μm	np nd	np 24–27/10 μm
Keel		sigmoid, apically torsioned	strongly sigmoid	sigmoid, slightly apically torsioned	sigmoid, different degrees of torsion	sigmoid	sigmoid, different degrees of torsion
Plastid(s)		nd	nd	two, axial	one, lobed	nd	one, plate-like

*nd: not defined.

*np: not present.

formed of elliptical, finely perforated areolae continuing to the raphe canal, arched and reinforced with raphe fibulae (Fig. 45, KF = keel fibulae white arrows; RF = raphe fibulae, black arrows). Transapical striae on valve body uniseriate, 27–35 in 10 µm, with elliptical areolae (48–54 in 10 µm) occluded by finely perforated hymenes (Figs 48–50). Valvocopulae perforated with two rows of elongated areolae, smaller advalvar and larger abvalvar (Fig. 50). Cingulum composed of 6–8 open, crossed bands (Fig. 34).

Ecology: *Entomoneis paludosa* is widely distributed along the east and west coasts of Sweden, where habitats vary from slightly brackish in the northern parts of the Baltic Sea, to marine at the Kattegat and Skagerrak bays connected to the North Sea. It was found free living on sediments as well as epiphytic on a number of macrophytes.

Discussion

Overall, the morphology of *E. grisslehamnensis* and *E. paludosa* is congruent with *Entomoneis*, i.e., these species are panduriform in girdle view, they possess elevated bilobed, winged keel with sigmoid canal raphes and numerous intercalary girdle bands. The greatest morphological resemblance with other species is between *E. grisslehamnensis* and *E. aequabilis*, *E. decussata*, *E. paludosa*, *E. tenera* and *E. punctulata*. A detailed morphological comparison of the most important shared features is given in Table 1. On the other hand, several unique morphological features distinguish *E. grisslehamnensis* from these taxa. Most importantly, *E. grisslehamnensis* possesses pronounced, unequally distributed, elevated virgae in the winged keel, which separate 2–5 transapical valve body striae, clearly visible in girdle view (Figs 2–4), while virgae in similar species are equidistant, usually separating pairs of striae (Osada & Kobayasi 1985, Osada & Kobayasi 1990a, 1990b, Al-Handal et al. 2020). Valve apices of *E. grisslehamnensis* (in girdle view) are scalpelliform, like *E. tenera* or *E. aequabilis*, but these species differ from *E. grisslehamnensis* in outline and structure of the valve body to keel transition (basal fibulae absent and no visible line separating valve body and winged keel in *E. aequabilis*, and a straight to slightly arcuate outline formed by basal fibulae in *E. tenera*). Additionally, the structure of the transapical striae (perforated hymen with rectangular perforations in *E. tenera* but with short lines in *E. aequabilis*) shows greater divergence between *E. grisslehamnensis* and related species (Osada & Kobayasi 1991, Mejdandžić et al. 2017). Apex shape in the generitype *E. alata* (Ehrenberg 1845) Ehrenberg and *E. punctulata*, *E. paludosa* and *E. decussata* differs from that in *E. grisslehamnensis*, ranging from acute to protracted and acuminate apices (Osada & Kobayasi 1985, 1990b, 1990c). Linear to linear-lanceolate valves are typical for *Entomoneis*, seen in *E. alata*, *E.*

japonica, *E. annagodheae*, *E. punctulata* and *E. paludosa* as well as *E. grisslehamnensis*.

Entomoneis grisslehamnensis has a single plate-like plastid (Fig. 1), a feature shared with other species such as *E. tenera*, *E. pusilla* and *E. gracilis* (Mejdandžić et al. 2018). However, the valve structure of *E. grisslehamnensis* is markedly different from these taxa but more similar to species with two plastids (e.g., *E. paludosa*, *E. alata*, and *E. pulchra* (Bailey) Reimer). The shape and structure of areolae in *E. grisslehamnensis*, i.e., quadrangular, rarely rounded, equidistant and of similar size over most of the valve surface (Figs 30–33) is distinctive and not shared with other *Entomoneis* of similar frustule and valve outline and size. Areolae are rounded in *E. alata*, elliptical and enclosed with finely perforated hymenes in *E. paludosa*, rounded and of variable size and arrangement in *E. annagodheae*, striae closed by perforated hymenes with linear perforations in *E. punctulata* and apically elongated in *E. triundulata* (Osada & Kobayasi 1990a, 1990b, Liu et al. 2018, Al-Handal et al. 2020). The silica deposition (a rim) on the walls of wing areolae (Fig. 32), which appear as scattered tiny dots in LM, was observed in all examined cells from both locations and seems to be another unusual feature of *E. grisslehamnensis*. These dots differ from those seen in *E. alata* (first described by Cleve 1894) and considered a distinguishing feature between *E. alata* and *E. paludosa* (Patrick & Reimer 1975), characterized as fibulae positioned on the wing virgae (Osada & Kobayasi 1985).

Another common feature of *Entomoneis* is the sigmoid raphe canal positioned on an elevated bilobed keel. According to Liu et al. (2018), two groups of *Entomonies* valves can be recognized based on the sigmoid keel orientation (external valve view); the first with a 2-shaped keel outline, the second an S-shaped keel outline. Liu et al. (2018, Table 1, p. 251) stated that both valves of a frustule have the same orientation, but based on our observations and many other previously published studies, the orientation of the sigmoid keel is not the same on both valves of a frustule (epitheca and hypotheca), but merely a mirror-image, seen as S-shaped on one valve, and consequently 2-shaped on the other. For example, two ‘types’ of keel shapes can be observed in *E. annagodeae* (Al-Handal et al., 2020, Figs 13, 14, 16); *E. pusilla* (Mejdandžić et al. 2018, Fig. 2A, D); *E. infula* (Mejdandžić et al. 2018, Fig. 5B, C); *E. umbratica* (Mejdandžić et al. 2018, Fig. 7B, C). Similarly, as observed in the present study, *E. grisslehamnensis*, exhibited both types of keel curvature (Figs 8, 23, 24). Furthermore, if ‘types’ of keel curvature are to be used as a discriminating feature they must be consistent within a taxon. Liu et al. (2018) clearly missed that in describing *E. triundulata*, as this species has both types of curvature in published images (Liu et al., Figs 13–18 for 2-shaped, and Figs 20–26 for S-shaped). To conclude, we propose that this morphological feature is not used in the identification and/or separation of *Entomoneis* species.

Entomoneis grisslehamnensis appeared at two sites as two populations but was not observed in any other samples from other locations along the Baltic coast of Sweden. The population found in Grisslehamn was smaller in size, 43–66 µm long and 6–7.5 wide, while the population in Juniskär was characterized by larger frustules, 65–166 µm long and 7–10.5 µm at the central constriction. The cell structure of both populations was identical but cells of the two size groups were not observed together, therefore we consider that they are different morphotypes. The distance between these locations is 344 km with a shift in salinity from 1.3 at Juniskär to 4.9 at Grisslehamn. Considering the sampling time which was in two successive dates with no noticeable difference in temperature, salinity was the only measured factor that exhibited a significant change (3.6 difference). Although change in diatom cell size with salinity is not well documented, a few studies from the Baltic coast showed that a change of one salinity unit led to 32% increase in community volume (Svensson *et al.*, 2014), or that larger cells were a response to salinity (Snøeijis *et al.* 2002). Additionally, a few studies reported changes in diatom cell size and biovolumes in cultivated material, such as *Thalassiosira weissflogii* (Grunow) Fryxell & Hasle and *Cylindrotheca closterium* (Ehrenberg 1845) Reimann & Lewin (García *et al.* 2012, Novosel *et al.* 2022).

Entomoneis paludosa is one of the commonest, widely distributed, and problematic species of the genus. Misidentification is likely to occur in LM observations due to its similarity with some of its varieties, as well as with *E. alata* or *E. japonica* (*E. alata* var. *japonica* (Cleve) Osada) whose type material has not yet been re-examined (Osada & Kobayasi 1985). For instance, the species named *Entomonies* cf. *paludosa*, illustrated with LM and SEM images in Podunay *et al.* (2021), does not belong to this species based on type material examined by Dalu *et al.* (2015). Similarly, the images for *E. paludosa* presented in Witkowski *et al.* (2000, pl. 109, Figs 26, 27) look dubious and may belong to a different species. Other non-taxonomic publications have also misidentified this taxon (e.g., Jauffrais *et al.* 2017, Bedoshvili *et al.* 2021). The species named *E. paludosa* var. *paludosa* found in Japan (Osada & Kobayasi 1990c) also shows structural variation from type material. These authors observed a raphe canal composed of two tubular canals stacking over each other, separated by a row of fibulae (Osada & Kobayasi 1990c, Figs 18–20). The raphe canal of type material of *E. paludosa* is a single tubular canal (W. Smith's type material and additional specimens from the Kowie River examined by Dalu *et al.* 2015), also found in the material examined in this study. Furthermore, a recent study by Long *et al.* (2022) found *E. paludosa* in fresh to slightly brackish water Lake Qinghai which also appears to have single tubular raphe canal. However, Long *et al.* (2022) failed to recognize variation in the outline of the transition between valve body and wing formed by basal fibulae

(feature visible in LM), easily observed from the comb-like hymenate striae found on the elevated wing, that is clearly present in this dubious species. Consequently, the authors described a new species, *E. qinghainensis*, which 'differs' from *E. paludosa* in the shape of this outline and its distance from raphe canal (i.e., length of the regular areolar wing striae proximal to the raphe canal). As Dalu *et al.* (2015) have shown, and as we present here, variation in shape of transition between valve body and wing, is directly related to size variation in *E. paludosa*. Larger cells have a sinusoidal apical outline, with a more or less straight central part, but smaller cells usually have a more bent sinusoidal apical outline and bi-sinusoidal central part (observed in girdle view; central part constricted). Additionally, larger cells have longer wing striae, while smaller cells have shorter, irregularly outlined comb-like hymenate wing striae (Dalu *et al.* 2015; this study). Therefore, we strongly support the argument that *E. paludosa* shows plasticity in these features (transition outline, length of comb-like hymenate striae, and wing striae) and that the main identification characters should be its size range (valve length 40–130 µm, valve width 20–50 µm), number of valve striae (21–35 in 10 µm), presence of comb-like hymenate striae and ultrastructure of elliptical areolae and girdle bands.

The material of *E. paludosa* examined in this work came from several locations along the Swedish coasts, representing brackish and marine habitats. The ultrastructure of *E. paludosa* valves illustrated here are congruent with W. Smith's type material and specimens from the Kowie River examined by Dalu *et al.* (2015). These include the transition between valve and keel, continuous comb-like hymenate striae with fine perforations (comb-like structure) on the wings, uniseriate striae on the valve body with elliptical areolae occluded by finely perforated hymenes, wide raphe canal with raphe fibulae and uniseriate transapical striae on wing area proximal to the raphe canal. Additionally, these features and measurements are congruent with Long *et al.*'s (2022) observations made on *E. paludosa* from Lake Qinghai, as well as *E. qinghainensis*, which we believe represents either *E. paludosa* or a variety of *E. paludosa* (Long *et al.* 2022). Furthermore, Long *et al.* (2022) proposes that hymenate striae are referred to as rices (Osada & Kobayasi 1990c) or hymen strips (Long *et al.* 2022). These are found in *E. alata*, *E. aequabilis*, *E. punctulata*, *E. pseudoduplex*, *E. tenera*, *E. gracilis*, *E. pusilla*, *E. vilicicii*, *E. infula*, *E. umbratica*, *E. sinensis* and *E. qinghainensis* and can be separated into two types: hymenes with (i) round and (ii) with linear perforations. However, variation in pore appearance, as well as density and arrangement, suggest that they cannot be clearly designated as 'Type One' or 'Type Two'. The most obvious example is *E. paludosa*, which has hymenate striae in comb-like structures, perforated by very small, round and dense perforations, observed in detail with TEM for the

first time in this study. Unfortunately, Dalu et al. (2015) did not show details of these striae when they examined type material of *E. paludosa*.

To date, our knowledge of *Entomoneis* taxonomy remains limited. With only 32 taxonomically accepted species (and unknown numbers of future transfers from *Amphiprora* and generally undiscovered species), studies that provide detailed microscopical observations and/or phylogenetic studies of those species are critically important. It is crucial to emphasize that using TEM for fine detail observations in this genus allows researchers to observe some previously undocumented features, not even observed in type material (e.g., fine perforations in comb-like structure of *E. paludosa* wing). The use of both SEM and TEM allowed us to define unique features by which *E. grisslehamnensis* can be correctly identified: (i) irregularly spaced elevated virgae, (ii) quadrangular areolae with silicified rim and (iii) pronounced narrow raphe-canal with 3–4 areola long striae. TEM can also be more useful than SEM for studying weakly silicified species (mostly planktonic ones in this genus), and we consider it should be obligatory for morphological studies of *Entomoneis*. The description of *E. grisslehamnensis* and examination of wild material of *E. paludosa* included here contribute to this, and enrich our knowledge of the diatom flora of the Baltic Sea, and the Bacillariophyceae in general.

Acknowledgements

The authors are grateful to Mr. Mikael Hedblom, Department of Biological and Environmental Sciences, University of Gothenburg, for his help in sample collection and transport. The first author expresses his gratitude to Dr Stefan Gustafsson, Chalmers University, Gothenburg, Sweden for assisting with the SEM. We like to express our deepest gratitude to the Editor in Chief, Dr Eileen Cox, for very valuable comments and suggestions that greatly improved the manuscript. Author contributions: Adil Al-Handal: sampling, manuscript concept, light and electron microscopy, morphological analysis. Maja Mucko: manuscript concept, electron microscopy, morphological analysis. Peharec Štefanić Petra: TEM analysis. Angela Wulff: funding acquisition, supervision and supporting writing.

Disclosure statement

No potential conflict of interest was reported by the author(s).

Funding

This work is part of a project funded by the Swedish Research Council for Environment, Agricultural Sciences and Spatial Planning (FORMAS) as part of the project 2017-0085.

ORCID

Adil Y. Al-Handal  <http://orcid.org/0000-0003-4703-7823>

Maja Mucko  <http://orcid.org/0000-0002-7301-7888>

Petra Peharec Štefanić  <http://orcid.org/0000-0003-4889-6910>

Angela Wulff  <http://orcid.org/0000-0003-0015-7019>

References

- AL-HANDAL, A.Y., MUCKO, M. & WULFF, A. 2020. *Entomoneis annagodhei* sp. nov., a new marine diatom (Entomoneidaceae, Bacillariophyta) from the west coast of Sweden. *Diatom Research* 35: 269–279. doi:10.1080/0269249X.2020.1787229
- BEDOSHVILI, Y., PODUNAY, Y., NIKONOVA, A., MARCHENKOV, A., BAIRAMOVA, E., DAVIDOVICH, N. & LIKHOSHWAY, Y. 2021. Lipid and fatty acids accumulation features of *Entomoneis* cf. *paludosa* during exponential and stationary growth phases in laboratory culture. *Diversity* 13: 459.
- CLAVERO, E., GRIMALT, J.O. & HERNÁNDEZ-MARINNE, M. 1999. *Entomoneis vertebralis* sp. nov. (Bacillariophyceae); a new species from hypersaline environments. *Cryptogamie Algologie* 20: 223–234.
- CLEVE, P.T. 1894. Synopsis of the naviculoid diatoms. *Kongliga Svenska vetenskaps-akademiens handlingar* 26: 1–194.
- DALU, T., TAYLOR, J.C., RICHOUX, N.B. & FRONEMAN, P.W. 2015. A re-examination of the type material of *Entomoneis paludosa* (W Smith) Reimer and its morphology and distribution in African waters. *Fottea* 15: 11–25.
- EHRENBERG, C.G. 1845. *Neue Untersuchungen über das kleinste Leben als geologisches Moment*. Berlin Kurfürstlich-Brandenburgische Societät der Wissenschaften, Berlin, pp. 53–88.
- GARCÍA, N., LÓPEZ-ELÍAS, J. A., MIRANDA, A., MARTÍNEZ-PORCHAS, M., HUERTA, N. & GARCÍA, A. 2012. Effect of salinity on growth and chemical composition of the diatom *Thalassiosira weissflogii* at three culture phases. *Latin American Journal of Aquatic Research* 40: 435–440.
- GUIRY, M.D. & GUIRY, G.M. 2023. *Algaebase*. World-wide electronic publication, National University of Ireland, Galway.
- HÄLLFORS, G. 2004. *Checklist of Baltic Sea Phytoplankton Species (including some heterotrophic protistan groups)*. Baltic Sea Environment Proceedings vol. 95, 210 pp.
- JAUFFRAIS, T., AGOGUÉ, H., GEMIN, M. P., BEAUGEARD, L. & MARTIN-JÉZÉQUEL, V. 2017. Effect of bacteria on growth and biochemical composition of two benthic diatoms *Halamphora coffeaeformis* and *Entomoneis paludosa*. *Journal of Experimental Marine Biology and Ecology* 495: 65–74.
- JOHN, J. 1983. The diatom flora of the Swan River estuary Western Australia. *Bibliotheca Phycologica* 64: 359.
- KUYLENSTIERNA, M. 1990. *Benthic algal vegetation in the Nodre Älv Estuary (Swedish west coast)*. Ph.D. thesis, University of Gothenburg.
- LIU, B., WILLIAMS, D.M. & ECTOR, L. 2018. *Entomoneis triundulata* sp. nov. (Bacillariophyta), a new freshwater diatom species from Dongting Lake, China. *Cryptogamie Algologie* 39: 239–253.
- LONG, J.Y., WILLIAMS, D.M., LIU, B., MO, W.H. & QUAN, S.J. 2022. Ultrastructure of three species of *Entomoneis* (Bacillariophyta) from Lake Qinghai of China, with reference to the external areola occlusions. *PhytoKeys* 189: 29–50. doi:10.3897/phytokeys.189.78149.
- LOWE, R.L. 2003. Keeled and canalled raphid diatoms. In: *Freshwater Algae of North America, ecology and classification*. (Ed. by WEHR, J.D. & SHEATH R.G.), Academic press, San Diego. pp. 669–684.

- MEJDANDŽIĆ, M., BOSAK, S., ORLIĆ, S., GLIGORA UDOVIČ, M., PEHAREC ŠTEFANIĆ, P., ŠPOLJARIĆ, I., MRŠIĆ, G. & LJUBEŠIĆ, Z. 2017. *Entomoneis tenera* sp. nov., a new marine planktonic diatom (Entomoneidaceae, Bacillariophyta) from the Adriatic Sea. *Phytotaxa* 292: 1–18.
- MEJDANDŽIĆ, M., BOSAK, S., NAKOV, T., RUCK, E., ORLIĆ, S., GLIGORA UDOVIČ, M., PEHAREC ŠTEFANIĆ, P., ŠPOLJARIĆ, I., MRŠIĆ, G. & LJUBEŠIĆ, Z. 2018. Morphological diversity and phylogeny of the diatom genus *Entomoneis* (Bacillariophyta) in marine plankton: six new species from the Adriatic Sea. *Journal of Phycology* 54: 275–298.
- NOVOSEL, N., MIŠIĆ RADIĆ, T., LEVAK ZORINC, M., ZEMLA, J., LEKKA, M., VRANA, I., GAŠPAROVIĆ, B., HORVAT, L., KASUM, D., LEGOVIĆ, T., ŽUTINIĆ, P., GLIGORA UDOVIČ, M. & IVOŠEVIĆ DENARDIS, N. 2022. Salinity-induced chemical, mechanical, and behavioral changes in marine microalgae. *Journal of Applied Phycology* 34: 1293–1309.
- OSADA, K. & KOBAYASI, H. 1985. Fine structure of the brackish hwater pennate diatom *Entomoneis alata* (Ehr.) Ehr. var. *japonica* (Cl.) comb. nov. *Japanese Journal of Phycology* 33: 215–224.
- OSADA, K. & KOBAYASI, H. 1990a. *Entomoneis centrospinosa* sp. nov., a brackish diatom with raphe-bearing keel. *Diatom Research* 5: 387–396.
- OSADA, K., KOBAYASI, H. 1990b. Fine structure of the marine pennate diatom *Entomoneis decussata* (Grun) comb.nov. *Japanese Journal of Phycology* 38: 253–261.
- OSADA, K. & KOBAYASI, H. 1990c. *Observations on the forms of the diatom Entomoneis paludosa and related taxa*. Proceedings of the tenth International Diatom Symposium (Ed. by H. Simola, Koeltz Scientific Books, Koenigstein). 161–172.
- OSADA, K. & KOBAYASI, H. 1991. *Entomoneis aequabilis* sp. nov. (Bacillariophyceae), a brackish species without junction lines. *Japanese Journal of Phycology* 39: 157–166.
- PADDOCK, T.B.B. & SIMS, P.A. 1981. A morphological study of keels of various raphe-bearing 336 diatoms. *Bacillaria* 4: 177–222.
- PAILLÈS, C., BLANC-VALLERON, M. M., POULIN, M., CRÉMIÈRE, A., BOUDOUMA, O. & PIERRE, C. 2014. *Entomoneis calixasini* sp. nov., a new fossil diatom from the Turkish Marmara Sea sediments. *Diatom Research* 29(4): 411–422.
- PATRICK, R. & REIMER, C.W. 1975. *The diatoms of the United States*. Vol. II, part I. *Monographs of the Academy of Natural Sciences of Philadelphia* vol 13.
- PODUNAY, Y.A., DAVIDOVICH, N.A., DAVIDOVICH, O.I., WITKOWSKI, A., GASTINEAU, R. & SOLAK, C.N. 2021. The sexual reproduction and life cycle of the pennate diatom *Entomoneis* cf. *paludosa* (W. Smith) Reimer (Bacillariophyta). *Russian Journal of Marine Biology* 47: 19–28. doi: [10.1134/S1063074021010089](https://doi.org/10.1134/S1063074021010089)
- REINKE, D.C. & WUJEK, D.E. 2013. *Entomoneis reimeri* sp. nov., a new saline diatom species from Kansas. *Transactions of the Kansas academy of science* 116(3–4): 113–118.
- ROSS, R., COX, E.J., KARAYEVA, N.I., MANN, D.G., PADDOCK, T.B.B., SIMONSEN, R. & SIMS, P.A. 1979. An amended terminology for the siliceous components of the diatom cell. *Nova Hedwigia* 64: 513–533.
- ROUND, F.E. 1981. Some aspects of the origin of diatoms and their subsequent evolution. *BioSystems* 14(3–4): 483–486.
- ROUND, F.E., CRAWFORD, R.M. & MANN, D.G. 1990. *The diatoms, biology and morphology of the genera*. Cambridge University Press, Cambridge.
- RUCK, E.C. & THERIOT, E. C. 2011. Origin and evolution of the canal raphe system in diatoms. *Protist* 162(5): 723–737.
- SNOEIJIS, P., BUSSE, S. & POTAPOVA, M. 2002. The importance of diatom cell size in community analysis. *Journal of Phycology* 38(2): 265–281.
- SVENSSON, F., NORBERG, J. & SNOEIJIS, P. 2014. Diatom cell size, coloniality and motility: trade-offs between temperature, salinity and nutrient supply with climate change. *PLoS ONE* 9(10): e109993. doi:[10.1371/journal.pone.0109993](https://doi.org/10.1371/journal.pone.0109993)
- UTERMÖHL, V.H. 1931. Neue Wege in der quantitativen Erfassung des plankton. (Mit besonderer Berücksichtigung des Ultraplanktons.). *Internationale Vereinigung für Theoretische und Angewandte Limnologie: Verhandlungen* 5: 567–596.
- UTERMÖHL, V. H. 1958. Zur Vervollkommnung der quantitativen phytoplankton-methodik. *Internationale Vereinigung für Theoretische und Angewandte Limnologie: Mitteilungen* 9: 1–38.
- WILLIAMS, D.M. 2021. Names, taxa and databases: some aspects of diatom nomenclature. *Diatom Research* 36:101–106.
- WITKOWSKI, A., LANGE-BERTALOT, H. & METZELTIN, D. 2000. Diatom flora of marine coasts I. *Iconographia Diatomologica* 7: 1–925.